Data Valuation-Aware Coordinated Optimization of Power–Communication Coupled Networks Considering Hybrid Ancillary Services

Liya Ma, *Graduate Student Member, IEEE*, Hongxun Hui, *Member, IEEE*, and Yonghua Song, *Fellow, IEEE*

Abstract—The growth of renewable energies elevates the significance of maintaining system balance and imposes more demands on regulation resources. Flexible loads have been extensively regarded as prospective regulation resources for providing ancillary services within power networks, including frequency regulation, primary reserve, and synchronized reserve. However, the dispatch of flexible loads presents the challenges of frequent data transmission and explosive data volume, leading to substantial pressure on communication networks. To improve the communication performance for providing effective ancillary services, this paper proposes a coordinated optimization framework for dispatching flexible loads in data valuation-aware power-communication coupled networks. The framework employs: 1) a data valuation approach considering inherent characteristics and ancillary services to distinguish the data transmission preference; 2) an analogous model of communication networks to power networks, formulating the relationships between different components (e.g., nodes, branches, et al.) within coupled networks; and 3) a coordinated optimization model for coupled networks, which analyzes the impact of data valuation-aware transmission in communication networks on the dispatching of flexible loads in power networks. Numerical results demonstrate that the proposed coordinated optimization can effectively allocate regulation resources by considering the limitations of communication networks and significantly improve the regulation revenue engaged in hybrid ancillary services.

Index Terms—Power-communication coupled networks, data valuation, coordinated optimization, hybrid ancillary services.

NOMENCLATURE

Sets and Indices

$\mathcal{Q}_a/q_a$	Set/index of LA a's deviation data
$\mathcal{Q}_a^{\mathrm{C}}/q_a^{\mathrm{C}}$	Set/index of LA a's finally collected data
$\mathcal{Q}_a^{\mathrm{P}}/q_a^{\mathrm{P}}$	Set/index of LA a's inherently precise data
$\mathcal{A}/a$	Set/index of load aggregators

$\mathcal{G}/g$	Set/index of generators
$\mathcal{K}/k$	Set/index of communication branches
$\mathcal{L}/l$	Set/index of power branches
$\mathcal{W}/w$	Set/index of hybrid ancillary service scenarios

Abbreviations

BS	Base station
EB	Electricity bus
ICT	Information and communication technology
ISO	Independent system operator
LA	Load aggregator
PJM	Pennsylvania-Jersey-Maryland

Parameters

$\boldsymbol{\delta}^{-/+}$	$L \times 1$ vector of lower/upper bounds of bus angles
$\hbar_w$	$A \times 1$ vector of the relationship between regulation capacities and data-sending volumes for LAs
$\mathcal{J}^{\mathrm{A}}$	$G \times M$ unit-node incidence matrix of LAs
$\mathcal{J}^{\mathrm{G}}$	$G \times M$ unit-node incidence matrix of generators
$\mathcal{R}$	$1 \times W$ vector of requirements in hybrid scenarios
$\boldsymbol{\sigma}, \boldsymbol{\zeta}$	$K \times 1$ vectors of communication price parameters
$\boldsymbol{\tau}_w$	$1 \times M$ vector of regulation prices of all power nodes in scenario w
$\boldsymbol{B}^{\mathrm{F}}$	$I \times K$ node-branch incidence matrix in communication networks
$\boldsymbol{B}^{\mathrm{P}}$	$I \times K$ node-branch incidence matrix in power networks
$\boldsymbol{D}^{\mathrm{F},-/+}$	$K \times 1$ vector of lower/upper bounds for communication flow
$\boldsymbol{E}^{\mathrm{S}}/\boldsymbol{E}^{\mathrm{L}}$	$A \times I$ element-node incidence matrix of data source/load nodes
$\boldsymbol{k}_w^{\mathrm{Q}}/\boldsymbol{k}_w^{\mathrm{T}}$	$A \times 1$ vectors of weight coefficients of data quality/timeliness factor
$\boldsymbol{PR}^{\mathrm{D,G}}$	$G \times 1$ vector of generators' ramp rate limits
$\boldsymbol{P}^{\mathrm{D,A},-/+}$	$G \times 1$ vector of lower/upper bounds of LAs' dispatched load power
$\boldsymbol{P}^{\mathrm{D,G},-/+}$	$G \times 1$ vector of lower/upper bounds of generators' dispatched active power

$P^{\mathrm{F},-/+}$	$L \times 1$ vector of lower/upper bounds of active power flow
$P^{\mathrm{S,A}}$	$A \times 1$ vector of LAs' original load power
$P^{\mathrm{S,G}}$	$G \times 1$ vector of generators' original generation power
$Q^{\mathrm{D,G},-/+}$	$G \times 1$ vector of lower/upper bounds of generators' dispatched reactive power
$Q^{\mathrm{F},-/+}$	$L \times 1$ vector of lower/upper bounds of reactive power flow
$U^{-/+}$	$L \times 1$ vector of lower/upper bounds of bus voltages
ϕ_w	Dispatching period in scenario w
f_w	Data collection interval in scenario w
t_a^{rec}	Reception time
$M_{a,w}^{\mathrm{B}}$	Maximum permitted deviation of LA a

Variables

$\boldsymbol{\beta}_w^{\mathrm{Q}}$	$A \times 1$ vector of data quality factors in scenario w
$\boldsymbol{\beta}_w^{\mathrm{T}}$	$A \times 1$ vector of data timeliness factors in scenario w
$\boldsymbol{\delta}$	$M \times 1$ vector of electricity bus angles
$\boldsymbol{C}^{\mathrm{F}}$	$K \times 1$ vector of communication costs across K branches
$\boldsymbol{D}^{\mathrm{FinW}}$	$K \times W$ matrix of communication flow in W scenarios
$\boldsymbol{D}_w^{\mathrm{F}}$	$1 \times K$ vector of the communication flow in scenario w
$\boldsymbol{D}^{\mathrm{F}}$	$K \times 1$ vector of the communication flow
$\boldsymbol{D}_w^{\mathrm{L}}$	$A \times 1$ vector of data-receiving volumes of all data load nodes in scenario w
$\boldsymbol{D}_w^{\mathrm{NetS}}$	$A \times 1$ vector of all nodes' data-sending volumes in scenario w
$\boldsymbol{D}_w^{\mathrm{S\text{-}to\text{-}B}}$	$I \times K$ matrix of the allocated volume of branch k from node i
$\boldsymbol{D}_w^{\mathrm{S}}$	$A \times 1$ vector of data-sending volumes of all data source nodes in scenario w
$\boldsymbol{P}^{\mathrm{D,A}}$	$A \times 1$ vector of LAs' dispatched load power
$\boldsymbol{P}^{\mathrm{D,G}}$	$G \times 1$ vector of generators' dispatched generation power
$\boldsymbol{P}^{\mathrm{F}}$	$L \times 1$ vector of active power flow
$\boldsymbol{P}^{\mathrm{NetD}}$	$M \times 1$ vector of the nodal active power injection
$\boldsymbol{Q}^{\mathrm{F}}$	$L \times 1$ vector of reactive power flow
$\boldsymbol{Q}^{\mathrm{NetD}}$	$M \times 1$ vector of the nodal reactive power injection
$\boldsymbol{R}^{\mathrm{A}}$	$A \times W$ matrix of LAs' regulation power in hybrid scenarios
$\boldsymbol{R}^{\mathrm{G}}$	$G \times W$ matrix of generators' regulation power in hybrid scenarios
$\boldsymbol{R}_w^{A}$	$A \times 1$ vector of LAs' regulation capacities in scenario w
$\boldsymbol{U}$	$M \times 1$ vector of electricity bus voltages
$\boldsymbol{VoD}_w$	$A \times 1$ vector of LAs' data values in scenario w
$\boldsymbol{VoE}_w$	$A \times 1$ vector of LAs' external values in scenario w
$\boldsymbol{VoI}_w$	$A \times 1$ vector of LAs' internal values in scenario w

I. INTRODUCTION

A. Background

THE REMARKABLE surge in renewable energies has been ignited by net-zero commitments made by major countries worldwide [1], [2]. According to the International Renewable Energy Agency, the share of renewable energies in power generation is projected to reach 68% by 2030 [3]. The rapid expansion of renewable energies results in a significant increase in fluctuating power generation in power systems [4]. The fluctuation gives rise to an ongoing concern regarding the growing power imbalance between the supply and demand sides [5]. It follows that substantial regulation resources are required to maintain the power balance by providing ancillary services, such as frequency regulation, primary reserve, and synchronized reserve. Traditionally, regulation resources are typically supplied by thermal power plants and hydropower generators, among others. The regulation capacity of traditional generators may be insufficient in the near future, given that their contribution is limited due to the increasing presence of renewable energies [6]. To address the insufficiency of regulation resources, regulating flexible loads to provide hybrid ancillary services has emerged as an alternative and effective approach by employing advanced information and communication technologies (ICTs) [7].

The general flexible loads contain air conditioners [8], electric vehicles [9] and heat pumps [10], et al. This is due to their significant contribution to overall power consumption and their ability to energy storage. Each individual with a single flexible load possesses a much lesser capacity in comparison to the single traditional regulation resource. Hence, massive flexible loads should be aggregated as load aggregators (LAs) to provide ancillary services, thereby offering regulation capacities equivalent to those of traditional regulation resources [11]. Hui et al. [12] investigate heating, ventilation, and air conditioning to provide frequency regulation services and further reduce the energy cost in distribution networks. Jia et al. [13] aggregate air conditioners and electric vehicles to offer operating reserve capacities by the LA. Gu et al. [14] utilize hydrogen as energy storage for providing ancillary services, especially for power-to-hydrogen systems. For hybrid services, Shafie-Khah et al. [15] investigate a bi-level framework to dispatch electric vehicles to offer energy, reserve, and regulation services.

The implementation of various advanced ICTs is crucial for effectively dispatching large-scale flexible loads to provide hybrid services [16]. They encompass a range of options, from wireline to wireless networks, such as power line communications [17], fiber optics, and 5G, among others. For example, high-speed power-line communication technology is utilized in [18] to transmit and collect information on residual flexible loads in power systems. Haidar et al. [19] utilize power line communication to dispatch and control battery energy storage to provide regulation resources. Liang et al. [20] control the regulation resources in microgrids by WiFi, ZigBee, and cellular networks.

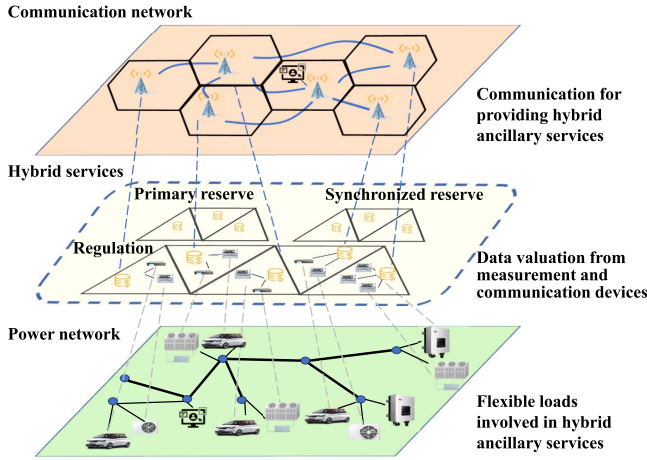Fig. 1 displays the regular dispatching process of large-scale flexible loads for providing hybrid services through

Fig. 1.   The regular dispatching process of large-scale flexible loads for providing hybrid services by utilizing advanced ICTs.

(a) Data volume before data valuation   (b) Data volume after data valuation

(c) The effect of higher data value   (d) The effect of lower data value

Fig. 2.   The impact of data valuation in power-communication coupled networks.

the utilization of advanced ICTs. In power networks, various flexible loads are aggregated by LAs to provide hybrid ancillary services, encompassing regulation, primary reserve, and synchronized reserve. Substantial measurement and communication devices, such as measurement terminals, and control units, are installed to monitor the data of distributed flexible loads. The data is transmitted to the independent system operator (ISO) through communication networks. More specifically, the data collected from aggregated flexible loads is forwarded by the base station and ultimately obtained by the ISO.

B. Motivations

The rapid expansion of distributed flexible loads poses significant challenges to communication networks:

i) While allowing for accurate and dependable dispatching results, increasing measurement and communication devices are considerably equipped to monitor the flexible loads' data, such as indoor temperatures of thermal loads, instructions of air conditioners, and load power. The utilization of numerous measurement equipment will inevitably result in vast quantities of data.

ii) Hybrid ancillary services necessitate a high frequency of data transmission to effectively monitor the data from flexible loads. For example, primary reserve and synchronized reserve services put forward that flexible loads should be monitored every minute within a 5-minute interval. More severally, regulation service demands that flexible loads should be monitored every 10 seconds within the same interval [21].

The explosive data volume and frequent data transmission impose critical pressure on communication networks, especially the non-negligible communication costs, which are necessary for dispatching large-scale flexible loads to provide hybrid ancillary services [22]. Being a vital element in power systems dispatching, it has been considered by several realistic power systems. In the Pennsylvania-Jersey-Maryland (PJM) region, the communication infrastructure incurs charges for every participant involved in their primary wide-area private network [23]. In the Australian Energy Market, the operator
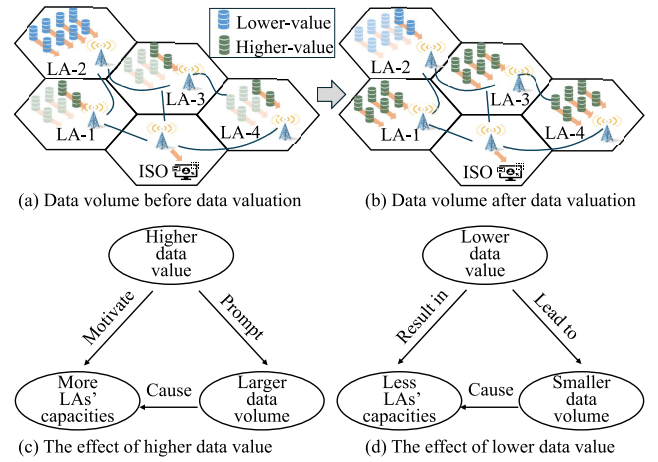
facilitates the availability of data communication providers for flexible loads to send data and receive instructions [24]. More specifically, various communication billing schemes have been proposed to charge for data transmission within communication networks. For example, Google Cloud implements a dynamically distributed price approach for transmitted data across different regions, with prices ranging from 0.10 USD/GB to 0.15 USD/GB [25].

There are several relevant papers on the communication network model for power networks. Liu et al. [26] propose a security assessment of communication networks on power networks. Considering inappropriate control commands, Xin et al. [27] further investigate the power-communication networks model to study the impact of communication security on power networks. Nevertheless, the communication network model is built for hierarchical power control systems. It may not be suitable for handling the transmission of explosive data volume when the ISO dispatches large-scale flexible loads in physical power networks. Moreover, there are some related papers on the optimization of power networks and communication networks. For instance, Ullah and Park [28] introduce the distributed energy trading strategy for directed communication networks. Han et al. [29] explore a collaborative optimization method for integrating the distribution power network and mobile communication network to utilize the flexibility of energy storage devices. However, the aforementioned studies neglect the existing communication costs in the operation of power networks. The dynamic communication prices and diverse data volumes in hybrid service scenarios result in communication expenses for the ISO in power networks.

Based on the critical pressure in data transmission in communication networks, organizing the data flow in communication networks can enhance communication performance, especially in communication cost savings by considering various values of LAs' data. With this approach, more valuable data is expected to be transmitted across communication networks, as illustrated in Fig. 2 (a) and (b). As shown in Fig. 2 (c), first, when the LAs process higher data values, they are expected to be dispatched more by the ISO in comparison

to those with lower data values. Second, a higher data value positively motivates larger data volume transmission across the communication networks. Third, a larger data volume typically results in increased LAs' regulation capacities. Conversely, a lower data value leads to smaller data volume transmission in Fig. 2 (d). A reduced data volume signifies less regulation capacities for LAs. Thus, the ISO is required to strike a balance among data value, data volume, and regulation capacities associated with dispatching large-scale flexible loads in the power-communication coupled networks.

However, during the dispatching process, the value of data varies depending on flexible loads and ancillary service scenarios [22]. On the one hand, in a given scenario, the data from diverse LAs possesses distinct inherent characteristics [30]. For example, due to variations in measurement devices across LAs, the coherence between the actual data and the meter data varies, resulting in the diverse data quality among LAs. Considering the varying reception time of data from LAs to ISO, the value attenuation differs among LAs, resulting in diverse data timeliness. Some researchers make explorations in this field. Wang et al. investigate the data inherent characteristics focusing on data distribution and present the data valuation approach for the solar power [31] and wind power [32]. Furthermore, Liu et al. perform data valuation based on data quality and data timeliness [33]. On the other hand, data valuation is related to the application scenarios [34]. In the power system, the data exhibits different economic values, depending on various ancillary services. Under the circumstance of identical data collection frequency, the economic value of data in the synchronized reserve service scenario surpasses that in the primary reserve service scenario. Therefore, the data value of flexible loads in hybrid services is a complex dynamic evaluation problem.

C. Contributions

To fill in this research gap, we propose a coordinated optimization framework for power-communication coupled networks incorporating data valuation to dispatch large-scale flexible loads in hybrid ancillary service scenarios, as shown in Fig. 1. In this framework, regulation resources with higher data value are prioritized for dispatch in power networks within hybrid ancillary services, i.e., w_1: the frequency regulation service; w_2: the primary reserve service; w_3: the synchronized reserve service. Simultaneously, the data from regulation resources with a higher data value, are also prioritized for transmission in communication networks. The contributions can be divided into three aspects:

1) We develop a data valuation approach that takes into account both internal and external values. The internal value is derived from inherent characteristics, i.e., data quality and timeliness. The external value is defined as economic values derived from regulation resource prices in hybrid ancillary service scenarios. The data valuation approach prioritizes the transmission of data in communication networks to address the escalating pressure caused by the massive volume of data being transmitted.

2) We establish the analogous model of communication networks to power networks to illustrate the element-to-element components in power-communication coupled networks. Nodes, branches, sources, flows, costs, and revenues are established analogously to elements in power networks. Innovatively, the communication network is established to facilitate the transmission of massive data volumes, enabling the ISO to dispatch large-scale flexible loads in power networks.

3) Based on power-communication analogous networks, we establish a data valuation-aware coordinated optimization strategy for the involvement of regulation resources in hybrid ancillary services. The ISO innovatively considers dynamic communication prices and the demands for transmitted data volume from hybrid service scenarios when dispatching large-scale flexible loads. By this approach, regulation capacities of regulation resources with flexible loads are reallocated by balancing the revenue and costs associated with regulation in power networks, as well as the revenue from data and the costs of communication in communication networks.

The rest of this paper is organized as follows. Section II develops a data valuation approach considering both inherent characteristics and hybrid ancillary services. Section III establishes an analogous model of data-transmitting communication networks. Section IV formulates the coordinated optimization problem that involves large-scale flexible loads in hybrid service scenarios. Section V validates the proposed strategy and displays the case results. Section VI concludes this paper.

II. DATA VALUATION MODEL

In the power-communication coupled networks, the data center gathers all the data from LAs to facilitate the dispatch outcomes by the ISO. Thus, the data center is the entity responsible for the process of data valuation. The diversity of data value in the dynamic power-communication coupled networks is contributed by two aspects:

1) The internal value, evaluated from the inherent data characteristics, includes data quality and data timeliness.

2) The external value, also known as the economic value derived from data application, is dependent on the price of the regulation power, which varies across different ancillary service scenarios.

Based on the current data asset pricing method [35], we develop the following data valuation approach by integrating both its internal value and external value:

$$\boldsymbol{VoD}_w = \boldsymbol{VoI}_w \odot \boldsymbol{VoE}_w, \ \ \forall w \in \mathcal{W}, \tag{1}$$

where the value of LAs' data for scenario w is represented by $A \times 1$ vector $\boldsymbol{VoD}_w = [VoD_{1,w}, \ldots, VoD_{A,w}]^T$. The internal value and the external value are represented by $A \times 1$ vectors $\boldsymbol{VoI}_w$ and $\boldsymbol{VoE}_w$, respectively. Symbols $\mathcal{W}$ and A represent the sets of ancillary service scenarios and the number of LAs, respectively.

A. Modeling of the Internal Value

The internal value refers to the inherent characteristics of data, including data quality and data timeliness. It can be

determined by:

$$VoI_w = k_w^Q \beta_w^Q + k_w^T \beta_w^T, \quad \forall w \in \mathcal{W}, \tag{2}$$

where VoI_w is the $A \times 1$ vector of internal values. The data quality factor is denoted by $A \times 1$ vector $\beta_w^Q = [\beta_{1,w}^Q, \ldots, \beta_{A,w}^Q]^T$. The data timeliness factor is denoted by $A \times 1$ vector $\beta_w^T = [\beta_{1,w}^T, \ldots, \beta_{A,w}^T]^T$. The parameters k_w^Q and k_w^T are the $A \times 1$ vectors of weight coefficients of data quality factor and data timeliness factor, respectively. They must satisfy $k_w^Q + k_w^T = \mathbf{1}_{A \times 1}$.

1) Data Quality Factor: There are multiple components involved in the data valuation process. The process covers the data generation by different units, the data measurement by acquisition devices, and the data transmission by ICTs. After undergoing multiple components, the data quality may be degraded between the inherently precise data before the process and the finally collected data after the process. Therefore, we establish the data quality factor as the level of coherence between these data sets. As the level of coherence increases, the data quality will improve [33]. We assume there are two data sets (inherently precise data $\mathcal{Q}_a^P$ and finally collected data $\mathcal{Q}_a^C$) for LA a ($\forall a \in \mathcal{A}$). The deviation among data sets will lead to the incoherence, represented by:

$$q_a = q_a^P - q_a^C, \quad \forall q_a \in \mathcal{Q}_a, \ q_a^P \in \mathcal{Q}_a^P, \ q_a^C \in \mathcal{Q}_a^C, \tag{3a}$$

where q_a^P and q_a^C are the elements belonging to datasets $\mathcal{Q}_a^P$ and $\mathcal{Q}_a^C$, respectively.

The data quality factor is defined as the probability of coherence within a specific threshold, as represented by:

$$E(M_{a,w}^B) = \int_0^{M_{a,w}^B} f(q_a) dq_a,$$
$$\beta_{a,w}^Q = E(M_{a,w}^B), \quad \forall a \in \mathcal{A}, \ \forall w \in \mathcal{W}, \tag{3b}$$

where $f(q_a)$ indicates the probability density function (PDF). The integral variable is denoted by q_a. The threshold M_a^B is the maximum permitted deviation of LA a. It should be noted that data quality factors are not affected by particular scenarios due to the inherent characteristics of the data.

It is well noted that the PDF varies according to the distribution. In this paper, we assume the deviation data follows the normal distribution.[1] Thus, the PDF can be expressed as:

$$f(q_a) = \frac{1}{\sqrt{2\pi}\sigma_a} e^{\frac{-(q_a - \mu_a)^2}{2\sigma_{a,N}^2}}, \tag{3c}$$

where μ_a and σ_a are the mean and standard deviation of the deviation dataset Q_a, respectively.

2) Data Timeliness Factor: The internal value of data will be deduced over the reception time t_a^{rec}, especially in the scenarios with high timeliness requirements. Thus, the data timeliness factor can be derived as:

$$\beta_{a,w}^T = \left(1 - \xi_w^T E(M_{a,w}^B)\right)^{t_a^{rec}}, \quad \forall a \in \mathcal{A}, \ \forall w \in \mathcal{W} \tag{4}$$

where $E(M_{a,w}^B)$ is involved in β_w^T to directly decide the attenuation rate $\xi_w^T E(M_{a,w}^B)$; $\xi_w^T \in (0, 1)$ is a coefficient of data

---

[1]The PDF varies according to the distribution. Other distributions are represented in the Appendix.

timeliness factor in the scenario w. It can be observed that the data timeliness factors vary across different service scenarios due to the difference of attenuation rate coefficients ξ_w^T.

B. Modeling of the External Value

Defined by its economic value, the external value of data varies when applied in different service scenarios. On the one hand, the economic value of data is strongly correlated with the trading prices of regulation resources in different ancillary service scenarios. For instance, if the data is utilized for dispatching large-scale flexible loads to provide the primary reserve, the economic value of data is derived from the clearing price in the ancillary service scenario of the primary reserve. It should be noted that the prices of ancillary service resources fluctuate across various service scenarios. The fluctuating prices of services positively contribute to the economic value of data. If the resources are more expensive in the frequency regulation scenario compared to the primary and synchronized reserve scenarios, the economic value of the data in the frequency regulation scenario surpasses that in the primary and synchronized reserve scenarios. On the other hand, the varying data collection frequencies also impact the economic value of data. Within a 5-minute interval, data from frequency regulation resources should be gathered every 10 seconds, whereas data from primary and synchronized reserve resources should be gathered every minute.

Thus, the external value is predominantly determined by the price of the corresponding resource and the data collection frequency in the specific service scenario, as represented by:

$$VoE_w = \frac{\chi}{\tau_w / f_w} p_w, \quad \forall w \in \mathcal{W}, \tag{5}$$

where $p_w = [p_{1,w}, \ldots, p_{A,w}]^T$ is the $A \times 1$ vector representing the unit trading price of regulation resources in ancillary service scenario w. The symbol χ is a unit conversion factor used to transform the unit from \$/MW to \$/GB, with the assumption that it is equal to 1. The denominator ϕ_w / f_w indicates the data collection frequency, where ϕ_w and f_w denote the dispatching period and data collection interval in the scenario w, respectively. It is noteworthy that the economic values of data are consistent across various LAs, as these parameters heavily rely on multiple ancillary services scenarios.

C. Discussion About the Developed Data Valuation Approach

The existing data valuation approaches can be classified into three aspects, i.e., the market-based model, the economic model, and the multi-dimensional model [30].

(1) The market-based model assesses the value of data through revenue generated from data sales, expenses incurred in data purchases, and the market capitalization of data-rich organizations. This model is commonly employed by organizations regularly engaged in the trading of data and data-centric enterprises.

(2) The economic model assesses the values of data based on its economic ramifications. This model is primarily used
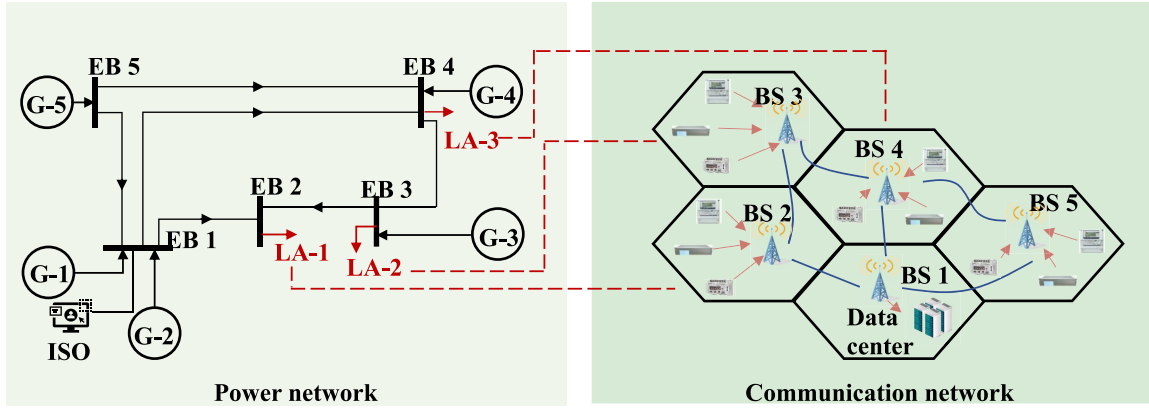
Fig. 3. The analogous model of communication networks to power networks.

by governments to evaluate the worth of making data public. For instance, governments share the weather data they obtain to aid in the sustainable advancement of weather forecasting ecosystems.

(3) The multi-dimensional model evaluates the values of data by assessing the internal characteristics of data and data application scenarios. This model employs formulas incorporating various dimensions to evaluate the value of data for business operations.

Given that the electricity data originates from respective sources and is transmitted to the ISO for dispatch, the multi-dimensional model is notably more suitable for valuing data in the power system compared to the other two models.

III. ANALOGOUS MODELING OF DATA-TRANSMITTING COMMUNICATION NETWORKS TO POWER NETWORKS

A. Coupling Modes of Power Networks and Communication Networks

To achieve coordinated optimization in power-communication coupled networks, we develop an analogous model of communication networks dedicated to data transmission. Analogous to the components in power networks, the communication networks are comprised of data source nodes, data load nodes, branches, and the topology. Fig. 3 presents the coupling mode of corresponding elements and parameters between power and communication networks.

All the analogous elements in communication networks indicate physical meanings, similar to power networks. First, in power networks, ISO dispatches large-scale flexible loads to serve as regulation resources in hybrid ancillary service scenarios. Analogously, in communication networks, the transmitted data is dispatched by the data center to support the dispatching results. Second, the fundamental elements of power networks consist of electricity buses and power branches, whereas communication networks are comprised of base stations and communication branches. Thereby, the node-branch incidence matrix of power networks is $\boldsymbol{B}^{\mathrm{P}}$ while the communication network's is $\boldsymbol{B}^{\mathrm{F}}$. Next, in power networks, regulation resources primarily originate from LAs, which aggregate large-scale flexible loads, whereas data sources are derived from base

stations, which collect data from measurement units in communication networks. By aggregating large-scale flexible loads through LAs, the regulation capacities $\boldsymbol{R}^{\mathrm{A}}$ are injected into nodes within power networks. Analogously, in communication networks, collected from measurement units, LAs' data with a volume of $\boldsymbol{D}^{\mathrm{A}}$ is injected into data nodes. As injection in power networks, regulation capacities are paid by scenario-based trading prices $\boldsymbol{\tau}_w$, leading to the regulation revenue $\mathcal{Q}_w^{\mathrm{P}}$ of LAs. As injection in communication networks, data volumes are paid by diverse data values $\boldsymbol{VoD}_w$. Finally, to transmit the substantial data resulting from the dispatching of flexible loads in communication networks, communication flow $\boldsymbol{D}^{\mathrm{F}}$ is considered equivalent to power flow $\boldsymbol{P}^{\mathrm{F}}$ in power networks. Consequently, in power-communication coupled networks with hybrid ancillary service scenarios, dispatching regulation resources takes into consideration regulation revenue $\mathcal{Q}_w^{\mathrm{P}}$, regulation costs $\mathcal{C}_w^{\mathrm{P}}$, data revenue $\mathcal{Q}_w^{\mathrm{D}}$, and communication costs $\mathcal{C}^{\mathrm{F}}$.

B. Analogous Modeling of Data Nodes

As power generators on the supply side and power loads on the demand side in power networks, data nodes can be analogously categorized as data source nodes and data load nodes in communication networks. As shown in Fig. 1, data source nodes send data in communication networks, which is generated by dispatching the LAs in hybrid scenarios. Data load nodes receive all the data injected by data source nodes.

1) Modeling of Data Source Nodes: The data-sending volume of LAs is dependent on the number of aggregated flexible loads, the categories of flexible loads, and the data collection frequency of ancillary service scenarios involved. For example, the regulation capacity of an industrial entity exceeds that of a residential entity. In one scenario, dispatching one LA with industrial flexible loads entities generates a larger volume of data compared to that with residential entities. For one LA involved in hybrid scenarios, dispatching an equivalent regulation capacity for frequency regulation generates a greater volume of data compared to that for primary reserve and synchronized reserve. Thus, the data-sending volume of all the data source nodes in the communication networks in the

scenario w can be derived by:

$$D_w^S = \hbar_w \odot R_w^A, \ \ \forall w \in \mathcal{W}, \tag{6}$$

where the relationship between the regulation capacities and the data-sending volumes for LAs is shown by $A \times 1$ vector $\hbar_w = [\hbar_{1,w}, \ldots, \hbar_{A,w}]^T$. The regulation capacities of LAs in the scenario w are shown by $A \times 1$ vector $R_w^A = [R_{1,w}^A, \ldots, R_{A,w}^A]^T$. The symbol $\odot$ means the Hadamard product operator by the element-by-element product of two matrices.

2) Modeling of Data Load Nodes: During the dispatching interval, the ISO receives all the data from LAs involved in hybrid scenarios with flexible loads. Therefore, the data demand from the ISO is defined as a data load node in communication networks. The data-receiving volume of data load nodes in the scenario w can be shown by:

$$D_w^L = \left[0, \ldots, D_{j,w}^L, \ldots, 0\right]^T, \ \ \forall w \in \mathcal{W}, \tag{7}$$

where $D_{j,w}^L$ indicates the data-receiving volume of the data load node at node j, satisfying $D_{j,w}^L = \hbar_w^T R_w^A$.

Therefore, the vector of all the nodes' data-sending volume can be transformed into:

$$D_w^{\text{NetS}} = \left(E^S\right)^T D_w^S - \left(E^L\right)^T D_w^L, \ \ \forall w \in \mathcal{W}, \tag{8}$$

where E^S and E^L are the $A \times I$ element-node incidence matrices of data source nodes and data load nodes, respectively. The element $E_{a,i}^S$ and $E_{a,i}^L$ indicates if there is a data source or load at node i. The multipliers $(E^S)^T D_w^S$ and $(E^L)^T D_w^L$ thereby present the $I \times 1$ vectors of the nodal data-sending volume and nodal data-receiving volume, respectively.

Furthermore, the total net data source at all nodes can be denoted by $I \times W$ matrix $D^{\text{NetS}} = [D_1^{\text{NetS}}, \ldots, D_w^{\text{NetS}}]$.

C. Analogous Modeling of Communication Flow

1) Modeling of Data Traffic: All the injected data is carried through communication branches, resulting in data traffic within communication networks. Equivalent to power flow in power networks, the data traffic in communication networks is referred to as communication flow. It can be represented by the $1 \times K$ vector D_w^F:

$$D_w^F = \mathbf{1}_I D_w^{\text{S-to-B}}, \ \ \forall w \in \mathcal{W}, \tag{9a}$$

where the data traffic in the scenario w is derived by matrix $D_w^{\text{S-to-B}} = \{D_{i,k,w}^{\text{S-to-B}}\}_{I \times K}$, where the elements $D_{i,k,w}^{\text{S-to-B}}$ is allocated to the k-th branch in the communication network from node i in the scenario w. $\mathbf{1}_I$ is the $1 \times I$ vector with all ones.

Further, the communication flow in communication branches is denoted by a $K \times 1$ vector $D^F = [D_1^F, \ldots, D_K^F]^T$:

$$D^F = D^{\text{FinW}} \mathbf{1}_W, \ \ \forall k \in \mathcal{K}, \tag{9b}$$

where the communication flow of all communications in scenarios is a $K \times W$ matrix $D^{\text{FinW}} = [D_1^F, \ldots, D_W^F]$. The symbol $\mathcal{K}$ is the set of communication branches. The symbol $\mathbf{1}_W$ is a $W \times 1$ column vector with all ones.

The communication flow D^F should satisfy the following lower and upper bounds:

$$D^{F,-} \le D^F \le D^{F,+}, \ \ \forall k \in \mathcal{K}, \tag{9c}$$

2) Modeling of Communication Costs: In accordance with the general communication charging strategy, the communication flow can be billed based on communication prices. The dynamic prices are distributed spatially among communication branches within communication networks. The price vector of communication branches can be expressed by:

$$p^F = \sigma \odot D^F + \zeta, \tag{10a}$$

where the price parameters are expressed by $K \times 1$ vectors $\sigma = [\sigma_1, \ldots, \sigma_K]^T$ and $\zeta = [\zeta_1, \ldots, \zeta_K]^T$, respectively.

Thus, the communication costs of communication branches are derived as $K \times 1$ vector:

$$C^F = \text{diag}(\sigma)\left(D^F \odot D^F\right) + \text{diag}(\zeta)\left(D^F\right), \ \ \forall k \in \mathcal{K}, \tag{10b}$$

D. Analogous Modeling of Communication Networks Topology

The relationship between data nodes and communication branches can be represented by a node-branch incidence matrix $B^F = \{B_{i,k}^F\}_{I \times K}$. The element $B_{i,k}$ indicates the relationship between the node i and the branch k, satisfying:

$$B_{i,k} = \begin{cases} 1 & \text{if } i \text{ is the data-sending node for branch } k; \\ -1 & \text{if } i \text{ is the data-receiving node for branch } k; \\ 0 & \text{if } i \text{ is not connected with branch } k. \end{cases} \tag{11a}$$

The nodal balance of communication flow can be satisfied as:

$$D^{\text{NetS}} \mathbf{1}_W - B^F\left(D^F\right)^T = \mathbf{0}_I, \ \ \forall w \in \mathcal{W}, \tag{11b}$$

where the first part $D^{\text{NetS}} \mathbf{1}_W$ is the vector of I nodes' data-sending volume in the communication network. The second part $B^F(D^F)^T$ is the net communication flow of I nodes in the communication network by considering all scenarios. The symbol $\mathbf{0}_I$ denotes the $I \times 1$ column vector with all zeros.

IV. COORDINATED OPTIMIZATION OF POWER-COMMUNICATION NETWORKS

A. Modeling of Power Networks

1) Power Constraints of Generators: In one interval, generators ramp up their output power to offer regulation capacities in hybrid ancillary service scenarios. The dispatched generation power of generators involved in the scenario w $P^{D,G} = [P_1^{D,G}, \ldots, P_G^{D,G}]^T$ can be calculated by:

$$P^{D,G} = P^{S,G} + R^G \mathbf{1}_W, \ \ \forall w \in \mathcal{W}, \tag{12a}$$

where $P^{S,G}$ is the $G \times 1$ vector of the original generation power vector of generators. The matrix $R^G = [R_1^G, \ldots, R_W^G]$ is the $G \times W$ matrix of regulation power of generators in hybrid scenarios, where the element $R_{g,w}^G \ge 0$. The parameters G and W are the number of generators and scenarios in power networks, respectively.

The generation power should satisfy the following constraints:

$$P^{D,G,-} \le P^{D,G} \le P^{D,G,+}, \tag{12b}$$

$$Q^{D,G,-} \le Q^{D,G} \le Q^{D,G,+}, \tag{12c}$$

$$-PR^{D,G} \le P^{D,G} - P^{S,G} \le PR^{D,G}, \qquad (12d)$$

$$-QR^{D,G} \le P^{D,G} - P^{S,G} \le QR^{D,G}, \qquad (12e)$$

where the parameters $P^{D,G,-}$ and $P^{D,G,+}$ are the vectors of lower and upper bounds of generation power, respectively. The vector $PR^{D,G}$ and $QR^{D,G}$ mean the ramp rate limit of generators' active power and reactive power, respectively.

2) Power Constraints of LAs: In one interval, LAs reduce their output power to offer regulation capacities in hybrid ancillary service scenarios. The dispatched load power of LAs w $P^{D,A} = [P_1^{D,A}, \ldots, P_A^{D,A}]^T$ can be calculated by:

$$P^{D,A} = P^{S,A} - R^A \mathbf{1}_W, \ \forall w \in \mathcal{W}, \qquad (13a)$$

where $P^{S,A}$ is the $A \times 1$ vector of the original load power of LAs. The matrix $R^A = [R_1^A, \ldots, R_W^A]$ is the $A \times W$ matrix of regulation power of LAs in hybrid scenarios, where the element $R_{a,w}^A \ge 0$. The parameter A is the number of LAs.

The dispatched load power of LAs should satisfy the following constraints:

$$P^{D,A,-} \le P^{D,A} \le P^{D,A,+}, \qquad (13b)$$

$$-R^{D,A} \le P^{S,A} - P^{D,A} \le R^{D,A}, \qquad (13c)$$

where the parameters $P^{D,A,-}$ and $P^{D,A,+}$ are the vectors of lower and upper bounds of load power of LAs, respectively. The vector $R^{D,A}$ means the ramp rate limit of LAs.

3) Regulation Power Constraints: The regulation power of generators and LAs should satisfy the requirements in hybrid scenarios, which is denoted by $1 \times W$ vector $\mathcal{R} = [\mathcal{R}_1, \ldots, \mathcal{R}_W]$:

$$\mathbf{1}_M \left(\mathcal{J}^G\right)^T R^G + \mathbf{1}_M \left(\mathcal{J}^A\right)^T R^A = \mathcal{R}, \qquad (14)$$

where $\mathcal{J}^G$ and $\mathcal{J}^A$ represent the $G \times M$ unit-node incidence matrix of generators and the $A \times M$ unit-node incidence matrix of LAs, respectively. The symbol $\mathbf{1}_M$ is $1 \times M$ vector with all ones. The element $R_{g,w}^G$ of the $G \times M$ matrix R^G indicates the regulation capacity of generator g in scenario w. The multiplier $(\mathcal{J}^G)^T R^G$ thereby presents the $M \times W$ matrix of the regulation capacities from generators of M nodes in W scenarios in power networks. Further, the first part $\mathbf{1}_M(\mathcal{J}^G)^T R^G$ means the $1 \times W$ vector of total regulation capacities from generators of all nodes in W scenarios in power networks. Relatively, the element $R_{a,w}^A$ of the $A \times M$ matrix R^A indicates the regulation capacity of LA a in scenario w. The multiplier $(\mathcal{J}^A)^T R^A$ thereby presents the $M \times W$ matrix of the regulation capacities from LAs of M nodes in W scenarios in power networks. Further, the first part $\mathbf{1}_M(\mathcal{J}^A)^T R^A$ means the $1 \times W$ vector of total regulation capacities from LAs of all nodes in W scenarios in power networks.

4) Power Flow Constraints: A decoupled linearized power flow model in [36] is utilized in this study. The power flow of power branches in the scenarios can be denoted by $L \times 1$ vector $P^F = [P_1^F, \ldots, P_L^F]^T$, $Q^F = [Q_1^F, \ldots, Q_L^F]^T$, which are represented by:

$$P^F = diag(Y_1) * B^P * U + diag(Y_2) * B^P * \delta,$$

$$Q^F = diag(Y_2) * B^P * U - diag(Y_1) * B^P * \delta, \qquad (15a)$$

where P^F and Q^F are active and reactive power by branches. The symbols Y_1 and Y_2 are the real part and imaginary part of the branch admittance vector $\mathcal{B}$, respectively, satisfying $\mathcal{B} = [B_1, \ldots, B_L]^T$. The symbol B^P is the $M \times L$ node-branch incidence matrix in power networks. The symbol $U]$ is the vector of the bus voltages, satisfying $U = [U_1, \ldots, U_M,$ constrained by:

$$U^- \le U \le U^+, \qquad (15b)$$

The symbol δ is the vector of the bus angles, satisfying $\delta = [\delta_1, \ldots, \delta_M]^T$, constrained by:

$$\delta^- \le \delta \le \delta^+. \qquad (15c)$$

5) Nodal Power Balance Constraints: The active and reactive power injection vectors of all nodes in power networks are derived by follows, respectively:

$$P^{NetD} = \left(\mathcal{J}^G\right)^T P^{D,G} - \left(\mathcal{J}^A\right)^T P^{D,A},$$

$$Q^{NetD} = \left(\mathcal{J}^G\right)^T Q^{D,G} - \left(\mathcal{J}^A\right)^T Q^{D,A}, \qquad (16a)$$

where the element $\mathcal{J}_{g,m}^G$ indicates if there is a generator at node m. And $\mathcal{J}_{a,m}^A$ indicates if there is an LA at node m. The multiplier $(\mathcal{J}^G)^T P^{D,G}$ thereby presents the $M \times 1$ vector of the nodal active generation power. The multiplier $(\mathcal{J}^A)^T P^{D,A}$ thereby presents the $M \times 1$ vector of the nodal active load power. The multipliers $(\mathcal{J}^G)^T Q^{D,G}$ and $(\mathcal{J}^A)^T Q^{D,A}$ present the $M \times 1$ vector of the nodal reactive generation power and the nodal reactive load power, respectively.

The active and reactive power balance for each node in power networks should be enforced by constraints as follows, respectively:

$$B^P P^F - P^{NetD} = \mathbf{0}_M,$$

$$B^P Q^F - Q^{NetD} = \mathbf{0}_M, \qquad (16b)$$

where 0_M is the $M \times 1$ column vector with all zeros.

6) Transmission Capacity Constraints: The transmission capacity constraints of power branches at scenario w are represented by:

$$P^{F,-} \le P^F \le P^{F,+},$$

$$Q^{F,-} \le Q^F \le Q^{F,+}, \qquad (17)$$

where $P^{F,-}$, $Q^{F,-}$, $P^{F,+}$ and $Q^{F,+}$ are the vector of lower and upper lower bounds of power flow, respectively.

B. Data Valuation-Aware Coordinated Optimization Problem

Fig. 3 depicts the coordinated optimization involving data valuation-aware power-communication coupled networks and hybrid ancillary service scenarios. On one hand, in a given scenario, data generated by dispatching flexible loads, with various values, is transmitted through communication networks. This leads to significant data-valuation-aware communication costs, which can have an impact on the dispatching outcomes of generators and LAs in power-communication coupled networks. On the other hand, in hybrid ancillary service scenarios, there are varying values and volumes of injected data. As a result, communication flows occur with

data-valuation-aware power-communication coupled networks, which can impact the regulation capacities of generators and LAs in hybrid ancillary service scenarios. Therefore, we develop a coordinated optimization strategy to dispatch the regulation capacities of generators and LAs in power-communication coupled networks while incorporating data valuation within hybrid ancillary services. Considering that the data valuation is conducted by the data center, it covers the data communication costs and receives the data revenue from the varies data values in communication networks. Accordingly, the ISO manages the electricity costs and regulation revenues from the power networks involved in hybrid service scenarios. The objective for the coordinated optimization of power-communication coupled networks is to maximize the net total revenue with hybrid ancillary service scenarios, which can be expressed by:

$$\max \mathcal{F} = \sum_{w \in \mathcal{W}} [\mathcal{Q}_w^G + \mathcal{Q}_w^P + \mathcal{Q}_w^D$$
$$- \mathcal{C}_w^G - \mathcal{C}_w^P - \mathcal{C}_w^F], \tag{18a}$$

where $\mathcal{F}^{ISO}$ is the net regulation revenue. The symbols $\mathcal{Q}_w^G$ and $\mathcal{Q}_w^P$ represent the regulation revenue of generators and LAs, respectively. The symbol $\mathcal{Q}_w^D$ is the revenue of data value. The symbols $\mathcal{C}_w^G$ and $\mathcal{C}_w^A$ are the regulation cost of generators and LAs, respectively. The symbol $\mathcal{C}_w^F$ is the communication cost in scenario w.

The revenue of generators in the scenario w is represented by:

$$\mathcal{Q}_w^G = \boldsymbol{\tau}_w \boldsymbol{R}_w^G, \ \forall w \in \mathcal{W}, \tag{18b}$$

where the regulation prices of all nodes in power networks are denoted by the $1 \times M$ vector $\boldsymbol{\tau}_w = [\tau_{1,w}, \ldots, \tau_{M,w}]$.

The revenue of LAs in the scenario w is represented by:

$$\mathcal{Q}_w^P = \boldsymbol{\tau}_w \boldsymbol{R}_w^A, \ \forall w \in \mathcal{W}. \tag{18c}$$

The revenue of data value in the scenario w is represented by:

$$\mathcal{Q}_w^D = [\boldsymbol{VoD}_w]^T \boldsymbol{D}_w^S, \ \forall w \in \mathcal{W}. \tag{18d}$$

The regulation cost of generators in the scenario w is represented by:

$$\mathcal{C}_w^G = \left(\boldsymbol{a}^G\right)^T \left[\boldsymbol{R}_W^G \odot \boldsymbol{R}_W^G\right] + \left(\boldsymbol{b}^G\right)^T \boldsymbol{R}_W^G, \ \forall w \in \mathcal{W}. \tag{18e}$$

where $\boldsymbol{a}^G$ and $\boldsymbol{b}^G$ are the parameter vectors of the regulation cost function of generators in all nodes, denoted by $\boldsymbol{a}^G = [a_1^G, \ldots, a_M^G]^T$ and $\boldsymbol{b}^G = [b_1^G, \ldots, b_M^G]^T$, respectively.

The regulation cost of LAs in the scenario w is represented by:

$$\mathcal{C}_w^P = \left(\boldsymbol{a}^A\right)^T \left[\boldsymbol{R}_w^A \odot \boldsymbol{R}_w^A\right] + \left(\boldsymbol{b}^A\right)^T \boldsymbol{R}_w^A, \ \forall w \in \mathcal{W}. \tag{18f}$$

where $\boldsymbol{a}^A$ and $\boldsymbol{b}^A$ are the parameter vectors of the regulation cost function of LAs in all nodes, denoted by $\boldsymbol{a}^A = [a_1^A, \ldots, a_M^A]^T$ and $\boldsymbol{b}^A = [b_1^A, \ldots, b_M^A]^T$, respectively.

The total communication cost is represented by:

$$\mathcal{C}^F = \boldsymbol{\sigma}^T \left(\boldsymbol{D}^F \odot \boldsymbol{D}^F\right)^T + \boldsymbol{\zeta}^T \left(\boldsymbol{D}^F\right)^T, \ \forall k \in \mathcal{K}. \tag{18g}$$

Therefore, the objective function (18) is constrained by the analogous model of data-transmitting communication networks in Eqs. (6) - (11), and regulation constraints of regulation resources in power networks in Eqs. (12) - (17). This objective function is a quadratic function with no cross terms. The Hessian matrix is semi-positive definite. All the constraints are affine functions. Especially for the power flow of branches, the linearized AC power flow [36] is adopted to decouple the voltage magnitudes and bus angles in the power networks. It follows that the proposed optimization problem is ultimately a convex quadratic programming problem, which can be efficiently solved by utilizing commercial solvers such as Gurobi [37].

V. CASE STUDIES

In case studies, we discuss the impact of data valuation power-communication coupled networks on the dispatching of flexible loads. The simulations are conducted on a desktop computer with Inter Core i7-10700 CPU and 16G RAM utilizing MATLAB 2022b with the YALMIP optimization toolbox.

The effectiveness of the proposed dispatching strategy is validated in 5-bus and 118-bus power-communication coupled networks through a comparison of **S1: Conventional strategy** and **S2: Proposed strategy**.

In the conventional strategy, the ISO dispatches large-scale flexible loads in the power networks under the assumption that the data related to dispatching can be transmitted across the communication networks without any charges. Moreover, the ISO in S1 neglects the impact of data value derived from dispatching data, consequently forfeiting potential data revenue. Mathematically, the objective function of the optimization model in S1 encompasses generators' regulation revenue and costs, as well as LAs' regulation revenue and costs in Eq. (19a).

$$\max \mathcal{F} = \sum_{w \in \mathcal{W}} \left[\mathcal{Q}_w^G + \mathcal{Q}_w^P - \mathcal{C}_w^G - \mathcal{C}_w^P\right], \tag{19a}$$

where $\mathcal{F}$ is the net regulation revenue. The symbols $\mathcal{Q}_w^G$ and $\mathcal{Q}_w^P$ represent the regulation revenue of generators and LAs, respectively. The symbol $\mathcal{Q}_w^D$ is the revenue of data value. The symbols $\mathcal{C}_w^G$ and $\mathcal{C}_w^A$ are the regulation cost of generators and LAs, respectively.

During the dispatching process in S1, communication costs caused by data transmission are disregarded in contrast to the proposed strategy S2. Nevertheless, it is noteworthy that communication charges do exist and should be carefully taken into account for the dispatch of large-scale flexible loads [24]. It follows that the comprehensive net revenue in S1 should encompass the communication costs but exclude data revenue, which can be presented as follows:

$$\max \mathcal{F} = \sum_{w \in \mathcal{W}} \left[\mathcal{Q}_w^G + \mathcal{Q}_w^P - \mathcal{C}_w^G - \mathcal{C}_w^P - \mathcal{C}_w^F\right], \tag{19b}$$

where $\mathcal{F}$ is the net regulation revenue. The symbols $\mathcal{Q}_w^G$ and $\mathcal{Q}_w^P$ represent the regulation revenue of generators and LAs, respectively. The symbols $\mathcal{C}_w^G$ and $\mathcal{C}_w^A$ are the regulation cost
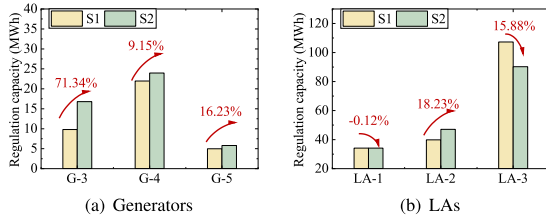
Fig. 4. Regulation capacities of generators and LAs in S1 and S2.

Fig. 5. Regulation capacities of units in each scenario in S1 and S2.

of generators and LAs, respectively. The symbol $\mathcal{C}_w^F$ is the communication cost.

In this paper, the proposed strategy integrates data with varying economic values and different internal values. The dispatching of flexible loads in power-communication coupled networks aims to achieve a balance between the net regulation revenue in power networks, and the data valuation-aware communication costs in communication networks. The objective function is presented in Eq. (18a). And it is the realistic total net revenue of the ISO in S2.

A. Coordinated Optimization Results of 5-Bus Power-Communication Coupled Networks

The topology of 5-bus power-communication coupled networks is based on the IEEE 5-bus test system in Fig. 3. In this paper, we consider each generator to provide one of the hybrid ancillary scenarios. Generator 3 provides frequency regulation in the scenario w_1, generator 4 provides primary reserve in the scenario w_2, and generator 5 provides synchronized reserve in the scenario w_3. Each LA can provide regulation resources to participate in hybrid service scenarios. The dispatching interval is one hour. The trading prices in hybrid ancillary scenarios come from the public data set in PJM [38]. All the units are price-takers. Besides, The communication pricing strategy refers to the public projects of giant industry companies, such as Alibaba and Google [25], [39].

1) The Impact Analysis of Data Valuation-Aware Power-Communication Coupled Networks: By considering multi-dimensional data values and dynamic communication prices in power-communication coupled networks, ISO will redistribute the regulation capacities in hybrid ancillary service scenarios among generators and LAs in S2 compared with S1. Fig. 4 compares the regulation capacities of generators and LAs in hybrid scenarios in S1 and S2. It is evident that all the generators enhance the regulation capacities to address the communication costs by dispatching LAs. Especially for generator 3, its regulation capacity increases by 71.34%, rising from 9.79 MWh in S1 to 16.78 MWh in S2. Furthermore, the generators 4 and 5 experience growth rates of 9.15% and 16.23%, respectively. Generators 1 and 2 are still working on their maximum generation power and have no extra regulation capacities. Instead, LAs decrease their total regulation capacities by 5.41% compared with S1. Although LA-2 enhances the regulation capacity by 18.23%, LA-1 and LA-3 reduce their overall regulation capacity in three scenarios by 0.12% and 15.88% to mitigate the communication costs, respectively.
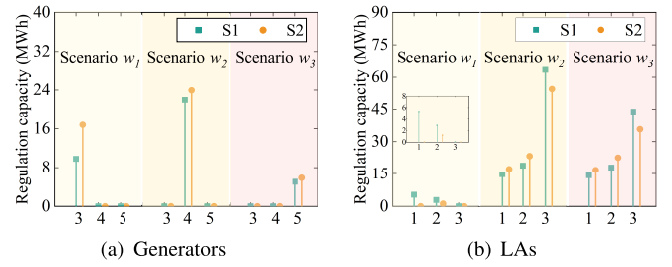
Last but not least, this paper investigates the coordinated optimization of power-communication coupled networks to dispatch large-scale flexible loads in advance. The coordinated optimization is conducted with a one-hour-ahead time frame. One of the main contributions of the proposed coordinated optimization framework is the communication network model that is equivalent to power networks, encompassing the communication-related objective function and constraints. There is no added complexity in the proposed coordinated optimization model for power-communication coupled networks. Based on the simulation results, the processing time of the proposed coordinated optimization model is 3.06 seconds, which is significantly lower than the one-hour ahead period. Furthermore, the computation time of 3.06 seconds for the coordinated optimization model proposed has a marginal increase of 5.52% compared to the 2.89 seconds of the conventional optimization model. It follows that the computation time is practical for dispatching large-scale flexible loads to provide hybrid services in the proposed coordinated optimization framework.

2) The Impact Analysis of Different Ancillary Services: Various data collection frequencies lead to varying data volumes in different ancillary scenarios, resulting in distinct data valuation-aware communication costs. To achieve the coordinated optimization of power-communication coupled networks with data valuation, the regulation capacities of generators and LAs can be reallocated in each scenario in Fig. 5. Compared with S1, each generator enhances its regulation capacity in the corresponding scenario, as depicted in Fig. 5(a). However, LAs reassign their regulation capacities in each scenario in Fig. 5(b). In the scenario w_1, all LAs decrease their regulation capacities due to the high data collection frequency for regulation service. In S1, LAs' and generators' total regulation capacities in scenario w_1 are 8.21 MWh and 9.29 MWh, respectively. In S2, LAs' and generators' total regulation capacities in scenario w_1 are 1.22 MWh and 16.78 MWh. Thus, LAs decrease the frequency regulation capacities of 6.99 MWh in S2 compared to S1. The share of LAs' regulation capacities in the total requirement of 18 MWh decreases from 45.59% in S1 to 6.77% in S2. This is a significant decrease in LAs' regulation capacities in scenario w_1 compared to 2.01% in scenario w_2 and 0.81% in scenario w_3. This is because the data volume collected in scenario w_1 is six times larger than that in scenario w_1 or scenario w_2 [21].

3) The Impact of Coordinated Optimization on Power-Communication Coupled Networks: Since the regulation
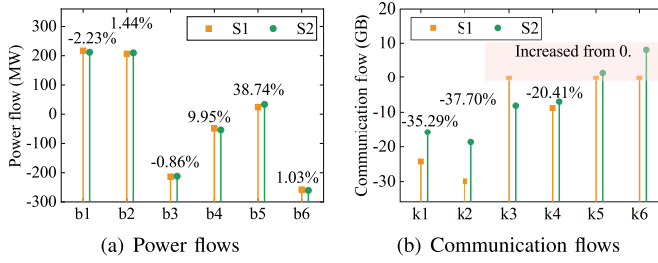
Fig. 6. Power flow and communication flows in power-communication coupled networks in S1 and S2.

TABLE I
OPTIMIZED DETAILED COSTS OF 5-BUS POWER-COMMUNICATION COUPLED NETWORKS

	S1 ($)	S2 ($)
Generators' costs	648.71	909.82
LAs' costs	4277.11	4058.79
Communication costs	435.65	237.13
Generators' revenue	2202.36	2868.18
LAs' revenue	10150.18	9484.36
Data value revenue	/	231.47
Total net revenue	6991.07	7378.27

capacities of generators and LAs are reallocated in power networks, the data-sending volume changes among data source nodes in communication networks. The adjustment of data volume results in the reassignment of communication flows within communication networks. Fig. 6 illustrates power flows and communication flows within the power-communication coupled networks in S1 and S2. As a result, the data volume resulting from dispatching flexible loads is reduced by 21.61%, decreasing from 54.14GB in S1 to 42.44 GB in S2. This reduction helps alleviate the burden of explosive data. Additionally, communication flows within branches k1, k2, and k4 decrease by 35.29%, 37.70%, and 20.41%, respectively, while maintaining their original data transmission directions. Specifically, communication flows within branches k3, k5, and k6 show an increase from a value of 0. This indicates the proposed strategy can effectively optimize communication flows within the coupled networks, resulting in a reduction in overall communication costs.

4) The Impact of Coordinated Optimization on Dispatching Cost and Revenue: Table I compares the detailed costs and revenues of generators and LAs in S1 and S2. The most obvious change is that the total net revenue increases by around 5.54% from 6991.07$ in S1 to 7378.27$ in S2. The realistic total cost decreases by 2.90% from 5361.47$ in S1 to 5205.74$ in S2 due to the improvement of communication costs. Besides, the proportion of communication costs to total costs decreases from 8.13% to 4.56% due to the reassignment of LAs' regulation capacities in hybrid scenarios. This improvement validates the effectiveness of the proposed coordinated optimization in power-communication coupled networks.

5) The Impact of Various Data Valuation Approaches: The value of data is developed based on three factors, i.e., data quality (F1), data timeliness (F2), and economic value (F3). The economic value depends on various scenarios while data quality depends on diverse LAs. And data timeliness is contributed by diverse LAs and various scenarios simultaneously.
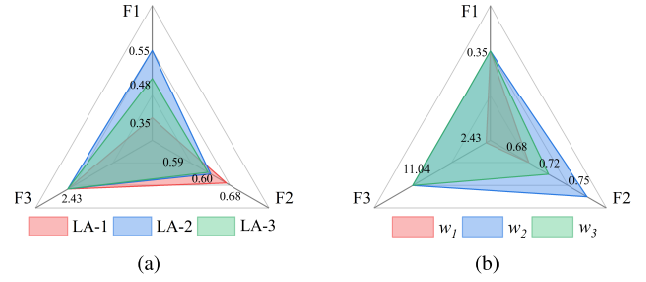

Fig. 7. The relationship among diverse data values, distributed LAs, and different service scenarios, where F1: data quality; F2: data timeliness; F3: economic value: (a) Data value factors of LAs in one scenario; (b) Data value factors of LA 1 in different service scenarios.
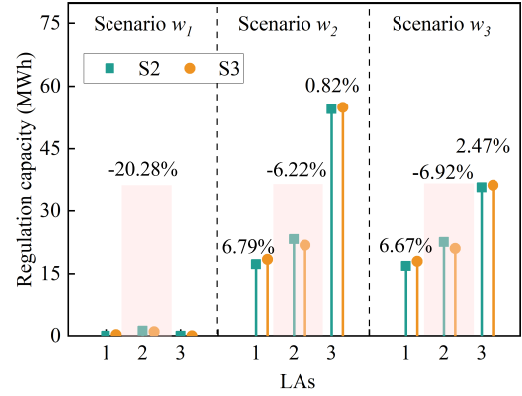

Fig. 8. Regulation capacities of LAs in each scenario in S2 and S3.

Fig. 7 illustrates the relationship among diverse data values, distributed LAs, and different service scenarios. Fig. 7(a) shows the distribution of LAs' data value in one scenario (w_1). Data quality factors vary among different LAs due to the diverse inherent characteristics of their data. For instance, LA-2 has the highest data quality factor of 0.55, whereas LA-1 has the lowest factor of 0.35. Despite having the lowest data quality, LA-1 has the highest data timeliness factor of 0.68, attributed to its minimal reception time. Additionally, in the given application scenario, i.e., ancillary service scenarios, the data economic value is contributed by the trading price and the frequency of data collection. Thus, in the scenario w_1 depicted in Fig. 7(a), all the LAs process an identical economic value of 2.43. However, in different service scenarios shown in Fig. 7(b), LA-1 exhibits various economic values across hybrid scenarios because of the diverse trading prices of regulation resources. Additionally, LA-1 exhibits the identical data quality factor in different service scenarios while presenting different data timeliness in various scenarios due to different requirements for different services.

Different data valuation approaches may affect the dispatching results of LAs in power-communication coupled networks within hybrid scenarios. Thus, we envision a desirable situation in S3, in which all LAs' data have equivalent inherent characteristics, including data quality and data timeliness. This situation can be considered that all the data is gathered from standardized devices and processes with precisely the same characteristics, ensuring the coherence of the data quality and

(a) Regulation capacities for generators in S1

(b) Regulation capacities for LAs in S1

(c) Regulation capacities for different nodes in S1

(d) Regulation capacities for generators in S2

(e) Regulation capacities for LAs in S2

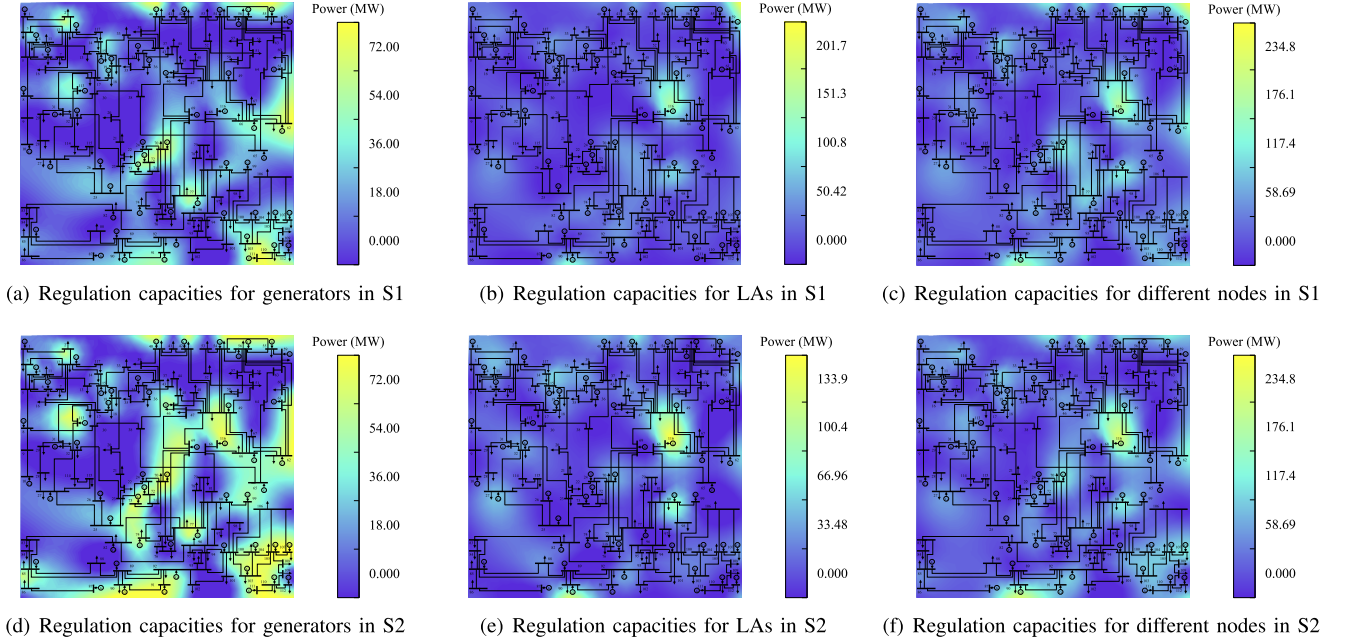(f) Regulation capacities for different nodes in S2

Fig. 9.   Regulation capacity for each unit in the 118-bus power-communication coupled networks in S1 and S2.

timeliness. Fig. 8 compares the regulation capacities of LAs in each scenario in S2 and S3. There are slight variations in LAs' regulation capacities in S3 compared to S2. For instance, LA-2 reduces its regulation capacity by 6.22% and 6.92% in the scenario w_2 and w_3, respectively. LA-3 enhances its regulation capacity by 0.82% and 2.47% in the scenario w_2 and w_3, respectively. Consequently, the diverse data valuation approaches affect the dispatching results of large-scale flexible loads in the power-communication coupled networks.

B. Coordinated Optimization Results of 118-Bus Power-Communication Coupled Networks

In this section, we further analyze the coordinated optimization involved with data valuation-aware on the 118-bus power-communication coupled networks. The power network is based on the IEEE 118-bus test system shown in Fig. 9.

Dynamic communication prices are distributed in the branches within communication networks, impacting the dispatching results of regulation resources in hybrid scenarios in power networks. Fig. 9 shows the regulation capacities of 54 generators and 99 LAs in the 118-bus power networks during a one-hour dispatching interval. The dispatching results by S1 in Fig. 9(a)-(c) and S2 in Fig. 9(d)-(f) are compared to discuss the impact of power-communication coupled networks on dispatching results of generators and LAs. Compared with S1, the total regulation capacities of generators increase significantly by 36.33% after taking into account data revenue and communication costs, while the overall regulation capacities of LAs tend to be lower. In terms of LAs, the top LA changes from LA-74 at bus 59 in S1 to LA-97 at bus 116 in S2, and the top regulation capacity of one LA decreases remarkably from 249.30MW to 165.60MW.
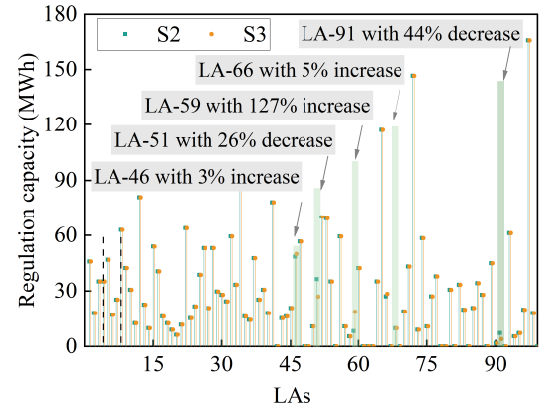

Fig. 10.   Regulation capacities of LAs in 118-bus power-communication coupled networks in S2 and S3.

Taking into account the essential communication costs with data valuation by dispatching flexible loads, the regulation capacities among diverse nodes in power networks are totally reallocated by the proposed coordinated optimization strategy. For instance, the top node with the most regulation capacity changes from bus 59 to bus 116.

To further discuss the impact of different data valuation approaches, we compare the regulation capacities of LAs in 118-bus power-communication coupled networks in S2 and S3 in Fig. 10. In S3, all the LAs have uniform inherent characteristics, i.e., equivalent-quality and equivalent-timeliness data. Economic value is the only factor varying with scenarios. By the data valuation approach in S3, approximately 94.95% of LAs maintain the regulation capacities compared to S2. Only five LAs, i.e., LA-46, LA-51, LA-59, LA-66, and LA-91, change their regulation capacities due to the impact of the

data valuation approach. LA-51 and LA-91 decrease their regulation capacity by 26% and 44%, respectively, while LA-46, LA-59, and LA-66 increase their extra regulation capacities by 3%, 127%, and 5%, respectively. It can be deduced that different data valuation approaches will influence the dispatching results of LAs as well.

VI. CONCLUSION

In this paper, we develop a data valuation-aware coordinated optimization framework for dispatching large-scale flexible loads in power-communication coupled networks. The main work is mainly contributed by: 1) the data valuation considering both inherent characteristics (i.e., data quality, data timeliness) and external values (i.e., economic value varying from hybrid services); 2) the analogous model of communication networks to power networks to formulate the relationships between the components in the coupled networks; 3) the coordinated optimization model integrating power flow and communication flow in coupled networks. Finally, numerical results present the effectiveness of the proposed framework. By considering the impact of data valuation in data-transmitting communication networks, the regulation capacities will be reallocated among regulation resources to provide hybrid ancillary services, effectively improving the regulation revenue in power-communication coupled networks.

APPENDIX

Here we consider three additional types of distributions as examples [31]. When the deviation data q_a follows the uniform distribution, the PDF can be expressed as:

$$f(q_a) = \frac{1}{\left(q_{a,\max,U} - q_{a,\min,U}\right)}, \tag{A1}$$

where $q_{a,\max,U}$ and $q_{a,\min,U}$ are the maximum value and minimum value of the deviation dataset Q_a, respectively.

When the deviation data q_a follows the logistic distribution, the PDF can be expressed as:

$$f(q_a) = \frac{e^{\frac{-(q_a - \mu_{a,L})}{\beta_{a,L}}}}{\beta_{a,L}\left[1 + e^{\frac{-(q_a - \mu_{a,L})}{\beta_{a,L}}}\right]^2}, \tag{A2}$$

where $\mu_{a,L}$ and $\beta_{a,L}$ are the location factor and shape factor.

When the deviation data q_a follows Laplace distribution, the PDF can be expressed as:

$$f(q_a) = \frac{1}{2\lambda_{a,LA}} e^{\frac{-|q_a - \mu_{a,LA}|}{\lambda_{a,LA}}}, \tag{A3}$$

where $\lambda_{a,LA}$ and $\mu_{a,LA}$ are location factor and shape factor.

REFERENCES

[1] (United Nat., New York, NY, USA). *For a Livable Climate: Net-Zero Commitments Must Be Backed by Credible Action*. Accessed: Nov. 2, 2023. [Online]. Available: https://www.un.org/en/climatechange/net-zero-coalition

[2] Y. Jiang, Z. Ren, and W. Li, "Committed carbon emission operation region for integrated energy systems: Concepts and analyses," *IEEE Trans. Sustain. Energy*, vol. 15, no. 2, pp. 1194–1209, Apr. 2024.

[3] (Int. Renew. Energy Agency, Masdar City, UAE). *Tripling Renewable Power and Doubling Energy Efficiency by 2030: Crucial Steps Towards 1.5 °C*. Accessed: Nov. 2, 2023. [Online]. Available: https://www.irena.org/Publications/2023/Oct/Tripling-renewable-power-and-doubling-energy-efficiency-by-2030

[4] S. Yang, K.-W. Lao, H. Hui, and Y. Chen, "Secure distributed control for demand response in power systems against deception cyber-attacks with arbitrary patterns," *IEEE Trans. Power Syst.*, early access, Mar. 24, 2024, doi: 10.1109/TPWRS.2024.3381231.

[5] X. Cai, N. Zhang, E. Du, Z. An, N. Wei, and C. Kang, "Low inertia power system planning considering frequency quality under high penetration of renewable energy," *IEEE Trans. Power Syst.*, vol. 39, no. 2, pp. 4537–4548, Mar. 2024.

[6] S. Wu, Q. Wang, Q. Chen, C. Yu, and Y. Tang, "Cyber-physical integrated planning of distribution networks considering spatial-temporal flexible resources," *Protect. Control Modern Power Syst.*, vol. 9, no. 3, pp. 142–156, 2024.

[7] H. Hui, Y. Ding, Q. Shi, F. Li, Y. Song, and J. Yan, "5G network-based Internet of Things for demand response in smart grid: A survey on application potential," *Appl. Energy*, vol. 257, Jan. 2020, Art. no. 113972.

[8] W. Cui et al., "Evaluation and sequential dispatch of operating reserve provided by air conditioners considering lead–lag rebound effect," *IEEE Trans. Power Syst.*, vol. 33, no. 6, pp. 6935–6950, Nov. 2018.

[9] H. Zhang, Z. Hu, Z. Xu, and Y. Song, "Evaluation of achievable vehicle-to-grid capacity using aggregate PEV model," *IEEE Trans. Power Syst.*, vol. 32, no. 1, pp. 784–794, Jan. 2017.

[10] Y. Zhao, J. Lin, Y. Song, and Y. Xu, "A hierarchical strategy for restorative self-healing of hydrogen-penetrated distribution systems considering energy sharing via mobile resources," *IEEE Trans. Power Syst.*, vol. 38, no. 2, pp. 1388–1404, Mar. 2023.

[11] D. Fan, S. Zhang, H. Huang, L. Zhou, Y. Wang, and X. Xiao, "Three-stage day-ahead scheduling strategy for regional thermostatically controlled load aggregators," *Protect. Control Modern Power Syst.*, vol. 8, no. 2, pp. 1–11, 2023.

[12] H. Hui et al., "A transactive energy framework for inverter-based HVAC loads in a real-time local electricity market considering distributed energy resources," *IEEE Trans. Ind. Informat.*, vol. 18, no. 12, pp. 8409–8421, Dec. 2022.

[13] H. Jia, Y. Ding, Y. Song, C. Singh, and M. Li, "Operating reliability evaluation of power systems considering flexible reserve provider in demand side," *IEEE Trans. Smart Grid*, vol. 10, no. 3, pp. 3452–3464, May 2019.

[14] Z. Gu, G. Pan, W. Gu, H. Qiu, and S. Lu, "Robust optimization of scale and revenue for integrated power-to-hydrogen systems within energy, ancillary services, and hydrogen markets," *IEEE Trans. Power Syst.*, vol. 39, no. 3, pp. 5008–5023, May 2024.

[15] M. Shafie-Khah, P. Siano, D. Z. Fitiwi, N. Mahmoudi, and J. P. S. Catalão, "An innovative two-level model for electric vehicle parking lots in distribution systems with renewable energy," *IEEE Trans. Smart Grid*, vol. 9, no. 2, pp. 1506–1520, Mar. 2018.

[16] M. Shafie-khah, P. Siano, J. Aghaei, M. A. Masoum, F. Li, and J. P. Catalão, "Comprehensive review of the recent advances in industrial and commercial DR," *IEEE Trans. Ind. Informat.*, vol. 15, no. 7, pp. 3757–3771, Jul. 2019.

[17] S. Galli, A. Scaglione, and Z. Wang, "For the grid and through the grid: The role of power line communications in the smart grid," *Proc. IEEE*, vol. 99, no. 6, pp. 998–1027, Jun. 2011.

[18] H. He, S. Cheng, Y. Zhang, and J. Nguimbis, "Home network power-line communication signal processing based on wavelet packet analysis," *IEEE Trans. Power Del.*, vol. 20, no. 3, pp. 1879–1885, Jul. 2005.

[19] A. M. Haidar, A. Fakhar, and K. M. Muttaqi, "An effective power dispatch strategy for clustered microgrids while implementing optimal energy management and power sharing control using power line communication," *IEEE Trans. Ind. Appl.*, vol. 56, no. 4, pp. 4258–4271, Jul./Aug. 2020.

[20] H. Liang, B. J. Choi, W. Zhuang, and X. Shen, "Stability enhancement of decentralized inverter control through wireless communications in microgrids," *IEEE Trans. Smart Grid*, vol. 4, no. 1, pp. 321–331, Mar. 2013.

[21] (PJM Interconnect., Norristown, PA, USA). *PJM Manual 12: Balancing Operations*. Accessed: Jul. 2, 2023. [Online]. Available: https://pjm.com/-/media/documents/manuals/m12.ashx

[22] J. Wang et al., "Data sharing in energy systems," *Adv. Appl. Energy*, vol. 10, Jun. 2023, Art. no. 100132.

[23] (PJM Interconnect., Norristown, PA, USA). *Metering System and Communication Requirements*. Accessed: Mar. 12, 2023. [Online]. Available: https://www.pjm.com/-/media/committees-groups/committees/mic/20170620-special/20170620-item-05-der-telemetry-metering-and-communication-requirements.ashx

[24] (AEMO, Melbourne, VIC, Australia). *Review of Power System Data Communication Standard*. Accessed: Mar. 12, 2023. [Online]. Available: https://aemo.com.au/consultations/current-and-closed-consultations/review-of-power-system-data-communication-standard

[25] "All networking pricing." Accessed: Mar. 12, 2023. [Online]. Available: https://cloud.google.com/vpc/network-pricing

[26] N. Liu, J. Zhang, H. Zhang, and W. Liu, "Security assessment for communication networks of power control systems using attack graph and MCDM," *IEEE Trans. Power Del.*, vol. 25, no. 3, pp. 1492–1500, Jul. 2010.

[27] S. Xin, Q. Guo, H. Sun, B. Zhang, J. Wang, and C. Chen, "Cyber-physical modeling and cyber-contingency assessment of hierarchical control systems," *IEEE Trans. Smart Grid*, vol. 6, no. 5, pp. 2375–2385, Sep. 2015.

[28] M. H. Ullah and J.-D. Park, "Distributed energy trading in smart grid over directed communication network," *IEEE Trans. Smart Grid*, vol. 12, no. 4, pp. 3669–3672, Jul. 2021.

[29] J. Han, N. Liu, and J. P. Catalão, "Optimization of distribution network and mobile network with interactive balance of flexibility and power," *IEEE Trans. Power Syst.*, vol. 38, no. 3, pp. 2512–2524, May 2023.

[30] M. Fleckenstein, A. Obaidi, and N. Tryfona, "A review of data valuation approaches and building and scoring a data valuation model," *Harvard Data Sci. Rev.*, vol. 5, no. 1, pp. 1–36, 2023.

[31] B. Wang, Q. Guo, T. Yang, and H. Sun, "Evaluation of information value for solar power plants in market environment," in *Proc. IEEE 4th Conf. Energy Internet Energy Syst. Integr. (EI2)*, 2020, pp. 3574–3580.

[32] B. Wang, Q. Guo, T. Yang, and B. Wen, "Value evaluation of wind power forecasting information for economic dispatch," in *Proc. 12th IEEE PES Asia-Pacific Power Energy Eng. Conf. (APPEEC)*, 2020, pp. 1–5.

[33] Z. Liu, X. Meng, Y. Liu, Y. Yang, and Y. Wang, "AUV-aided hybrid data collection scheme based on value of information for Internet of Underwater Things," *IEEE Internet Things J.*, vol. 9, no. 9, pp. 6944–6955, May 2021.

[34] M. Sajko, K. Rabuzin, and M. Bača, "How to calculate information value for effective security risk assessment," *J. Inf. Organ. Sci.*, vol. 30, no. 2, pp. 263–278, 2006.

[35] (China South. Power Grid, Guangzhou, China). *White Paper on Data Asset Management System*. Accessed: Jun. 22, 2023. [Online]. Available: http://www.chinapower.com.cn/dlxxh/jdtt/20210228/54736.html

[36] J. Yang, N. Zhang, C. Kang, and Q. Xia, "A state-independent linear power flow model with accurate estimation of voltage magnitude," *IEEE Trans. Power Syst.*, vol. 32, no. 5, pp. 3607–3617, Sep. 2017.

[37] "Gurobi optimizer reference manual." 2023. [Online]. Available: https://www.gurobi.com/

[38] (PJM Interconnect., Norristown, PA, USA). *Public Data*. Accessed: Aug. 8, 2023. [Online]. Available: https://dataminer2.pjm.com/list

[39] (Alibaba Cloud, Hangzhou, China). *Primary Traffic-Based Billing Scheme*. Accessed: Mar. 12, 2023. [Online]. Available: https://help.aliyun.com/document_detail/437187.html

Hongxun Hui (Member, IEEE) received the B.E. and Ph.D. degrees in electrical engineering from Zhejiang University, Hangzhou, China, in 2015 and 2020, respectively.

From 2018 to 2019, he was a Visiting Scholar with the Advanced Research Institute, Virginia Tech, and the CURENT Center, University of Tennessee. He is currently an Assistant Professor with the State Key Laboratory of Internet of Things for Smart City, University of Macau, Macau SAR, China. His research interests include optimization and control of power system, demand response, and Internet of Things technologies for smart energy.

Liya Ma (Graduate Student Member, IEEE) received the B.E. and M.E. degrees in electrical engineering from North China Electric Power University, Beijing, China, in 2019 and 2022, respectively. She is currently pursuing the Ph.D. degree in electrical and computer engineering with the University of Macau, Macau SAR, China.

Her research focuses on the coordinated optimization of power–communication coupling networks for dispatching large-scale flexible resources.

Yonghua Song (Fellow, IEEE) received the B.E. degree in electrical engineering from the Chengdu University of Science and Technology, Chengdu, China, in 1984, and the Ph.D. degree in electrical engineering from China Electric Power Research Institute, Beijing, China, in 1989.

From 1989 to 1991, he was a Postdoctoral Fellow with Tsinghua University, Beijing. He then held various positions with Bristol University, Bristol, U.K.; Bath University, Bath, U.K.; and John Moores University, Liverpool, U.K., from 1991 to 1996. In 1997, he was a Professor of Power Systems with Brunel University, where he has been a Pro-Vice Chancellor for Graduate Studies since 2004. In 2007, he took up a Pro-Vice Chancellorship and Professorship of Electrical Engineering with the University of Liverpool, Liverpool. In 2009, he was with Tsinghua University as a Professor of Electrical Engineering and an Assistant President and the Deputy Director of the Laboratory of Low-Carbon Energy. From 2012 to 2017, he was the Executive Vice President of Zhejiang University, as well as the Founding Dean of the International Campus and a Professor of Electrical Engineering and Higher Education of the University. Since 2018, he has been a Rector of the University of Macau, where he has also been the Director of the State Key Laboratory of Internet of Things for Smart City. His current research interests include smart grid, electricity economics, and operation and control of power systems.

Dr. Song was the recipient of D.Sc. by Brunel University in 2002, Honorary D.Eng. by the University of Bath in 2014, and Honorary D.Sc. by the University of Edinburgh in 2019. He was elected as the Vice-President of Chinese Society for Electrical Engineering (CSEE) and appointed as the Chairman of the International Affairs Committee of the CSEE in 2009. In 2004, he was elected as a Fellow of the Royal Academy of Engineering, U.K. In 2019, he was elected as a Foreign Member of the Academia Europaea.